

Glycyrrhizin protects human melanocytes from H₂O₂-induced oxidative damage via the Nrf2-dependent induction of HO-1

KUANHOU MOU^{1*}, WENJIE PAN^{2*}, DAN HAN¹, XIN WEN¹, FANG CAO^{3,4}, YI MIAO^{3,4} and PAN LI^{3,4}

¹Department of Dermatology, The First Affiliated Hospital of Xi'an Jiaotong University, Xi'an, Shaanxi 710061;

²Department of Orthopedic Surgery, Honghui Hospital, Xi'an Jiaotong University, Xi'an, Shaanxi 710054;

³Center for Translational Medicine; ⁴Key Laboratory for Tumor Precision Medicine of Shaanxi Province, The First Affiliated Hospital of Xi'an Jiaotong University, Xi'an, Shaanxi 710061, P.R. China

Received February 9, 2019; Accepted May 15, 2019

DOI: 10.3892/ijmm.2019.4200

Abstract. Oxidative stress serves a critical role in melanocyte death and is considered to be a major cause of vitiligo. The nuclear factor E2-related factor 2 (Nrf2) signaling pathway has an important role in the antioxidative stress mechanisms of melanocytes. Glycyrrhizin (GR) is a derivative of herbal medicines used to treat hepatitis and allergic disease due to its antiviral and anti-allergy effects. GR also activates Nrf2 and induces the expression of heme oxygenase (HO)-1 in macrophages. Whether GR can protect human melanocytes from oxidative stress remains unknown. The present study investigated the potential protective effects of GR against oxidative stress in human melanocytes and the mechanisms involved. Following exposure to 0.5 mM hydrogen peroxide (H₂O₂), human primary melanocytes were treated with 1 mM GR. Cell viability was determined using a Cell Counting Kit-8 assay, and apoptosis was evaluated by flow cytometry. GR treatment significantly improved cell viability, reduced the apoptotic rate of melanocytes and reduced the level of reactive oxygen species in human melanocytes. Furthermore, GR induced the nuclear translocation of Nrf2 and induced the expression of HO-1 in melanocytes. The knockdown of Nrf2 by small interfering RNA or the inhibition of HO-1 by ZnPP reversed the protective effect of GR on melanocytes against H₂O₂-induced cytotoxicity and apoptosis. These data demonstrate that GR protects human melanocytes from H₂O₂-induced oxidative damage via the Nrf2-dependent induction of HO-1, providing evidence for the application of GR in the treatment of vitiligo.

Introduction

The skin is the largest organ of the body and is the interface between the environment and internal milieu. The development of efficient sensory and effector capabilities to differentially react to changes in the external environment is a vital property of skin. Melanogenesis comprises a biosynthetic pathway under complex regulatory control by multiple factors (1). A key enzyme, tyrosinase, catalyzes the first and only rate-limiting steps in melanogenesis. The tyrosinase family genes TYR, tyrosinase related protein-1 and dopachrome tautomerase, responsible for pigmentation, are transcriptionally regulated by microphthalmia associated transcription factor (2). Within the context of the skin as a stress organ, the significance of melanogenesis extends beyond the assignment of a color trait. Melanin pigment serves a critical role in social communication and protection against the harmful effects of solar radiation (2). The lack of melanin pigment such as in vitiligo commonly affecting the face, can have significant psychological effects and impair the quality of life of the affected individuals. Due to their negative effect on physical appearance, conditions in which pigment is lacking may act as a potential barrier to social relationships and cause social anxiety. The lack of melanin pigment also makes the skin more sensitive to sunburn (3,4). Melanogenic activity serves as a unique molecular sensor and transducer of noxious signals and as a regulator of local homeostasis (5).

Vitiligo is a pigmentary disorder characterized by the selective destruction of melanocytes (6,7). To date, the cause of melanocyte death remains unknown. Evidence indicates that oxidative stress is a pivotal etiological aspect for the destruction of epidermal melanocytes in patients with vitiligo. Increased levels of reactive oxygen species (ROS) have been found in lesional and non-lesional skin *in vitro* and *in vivo* (8,9). The generation of ROS in melanocytes can disturb cell metabolism, proliferation and differentiation, which further induces autoimmune responses towards melanocytes, leading to their reversible cell damage (9,10).

The nuclear factor E2-related factor 2 (Nrf2) signaling pathway is important in the antioxidative stress mechanism of cells (11,12). Nrf2 is a transcription factor that is constitutively degraded through the ubiquitin proteasome pathway

Correspondence to: Dr Pan Li, Center for Translational Medicine, The First Affiliated Hospital of Xi'an Jiaotong University, 277 West Yanta Road, Xi'an, Shaanxi 710061, P.R. China
E-mail: imlipan@163.com

*Contributed equally

Key words: glycyrrhizin, nuclear factor E2-related factor 2, melanocyte, oxidative stress, heme oxygenase-1

under quiescent conditions. Nrf2-kelch-like ECH-associated protein 1 (Keap1) is an adaptor of the ubiquitin ligase complex that targets Nrf2 (13,14). Nrf2 is released from the Nrf2-Keap1 complex under oxidative stress and is transferred to the nucleus, where it binds to adenylate-uridylylate-rich elements and induces the release of downstream antioxidant genes. Such genes include heme oxygenase-1 (HO-1), NADH quinone oxidoreductase 1 (Nqo1), glutamate cysteine ligase catalytic subunit (Gclc) and glutamyl cysteine ligase modulator subunit (Gelm) (12,15). The Nrf2-keap1 signaling pathway serves a key role in protecting melanocytes from hydrogen peroxide (H_2O_2)-induced oxidative damage (16). Dysfunction of the Nrf2 signaling pathway increases the sensitivity of vitiligo melanocytes to H_2O_2 -induced oxidative damage (17). The knockdown of Keap1 in melanocytes promotes cell proliferation and survival. Keap1 silencing in melanocytes also induces melanogenesis through the HO-1-associated activation of β -catenin (18).

Glycyrrhizin (GR) is a natural compound in the roots and rhizomes of licorice. Previous studies have suggested that GR has anti-inflammatory, antiviral, antimicrobial, anticancer, immunomodulatory, hepatoprotective and cardioprotective effects (19-22). Studies have shown that GR serves an important role in the treatment of skin diseases. It ameliorates imiquimod-induced psoriasis lesions in mice (23). GR also ameliorates the symptoms of atopic dermatitis in the dinitrochlorobenzene-induced mouse model (24). GR induces melanogenesis by elevating the level of cAMP in b16 melanoma cells (25). Our previous study showed that combined therapy of orally administered GR and UVB improved active-stage generalized vitiligo (26). GR has also been reported to reduce oxidative stress by activating the Nrf2 pathway (27-29).

The effect of GR on vitiligo and whether GR can protect human melanocytes from oxidative stress remains unclear. The present study investigated the potential protective effect of GR against oxidative stress in normal human epidermal melanocytes (NHEMs) and the mechanisms involved. It was found that GR protected the NHEMs from H_2O_2 -induced oxidative damage via the Nrf2-dependent induction of HO-1, providing evidence for the application of GR in the treatment of vitiligo.

Materials and methods

Skin specimens and ethics statement. Skin specimens were obtained from six healthy male Chinese donors (mean age 6 years) who underwent circumcision in the Department of Urology of The First Affiliated Hospital of Xi'an Jiaotong University (Xi'an, China) between December 2017 and January 2018. The present study followed the guidelines of the Helsinki Declaration (1964) and subsequent amendments. The study was approved by the Research Ethics Board of the First Affiliated Hospital of Xi'an Jiaotong University. The guardians of all healthy donors provided written informed consent prior to inclusion in the study.

NHEM culture. Fresh tissues from children undergoing circumcision in the Department of Urology were obtained and digested for 16 h at 4°C with 0.25% dispase II (Roche Diagnostics, Indianapolis, IN, USA). The tissues were cut

into pieces and 0.25% trypsin was added, followed by incubation at 37°C for 30 min and subsequent centrifugation for 5 min at 800 x g at room temperature. The cell suspension was filtered through a 70- μ m cell strainer and seeded in a 10-cm cell culture dish at a density of $4-6 \times 10^6$ cells/ml. Melanocyte culture medium (Epilife Medium 254, Cascade Biologics/Invitrogen, Portland, OR, USA) containing human melanocyte growth supplement was added to the melanocyte culture, which was incubated at 37°C with 5% CO_2 . Primary melanocytes at passages three to eight were used in the present study.

Antibodies and reagents. The rabbit anti-human Nrf2 antibody (Abcam, Cambridge, MA, USA; cat. no. ab62352) and Alexa Fluor 488 goat anti-rabbit IgG (H+L) antibody (Invitrogen; Thermo Fisher Scientific, Inc., Waltham, MA, USA; cat. no. A-11008) were used. Analytical grade H_2O_2 was from Tianjin Chemical Reagent Factory (Tianjin, China). GR, propidium iodide (PI) and ZnPP were purchased from Sigma-Aldrich; Merck KGaA (Darmstadt, Germany).

Cell viability assay. Melanocyte viability was assessed using a CCK-8 cell proliferation test kit (KeyGen Biotech Co., Ltd., Nanjing, China), according to the manufacturer's instructions. Briefly, the primary melanocytes were seeded in 96-well plates at a density of 2.5×10^4 cells/well. H_2O_2 (0.5 mM) was added to the plates at room temperature. Morphological changes in the melanocytes were observed after 24 h with a Nikon Eclipse TS2 fluorescence microscope (Nikon Corporation, Tokyo, Japan). The medium was replaced together with 10 μ l/well cell proliferation and toxicity test solution, and the cells were cultured for 1-2 h at 37°C. The color change was monitored and measured at an absorbance at 450 nm using a microplate reader (Perkin-Elmer, Inc., Waltham, MA, USA).

ROS detection. The NHEMs were treated with 1 mM GR for 24 h in 6-well plates at a density of 1×10^6 cells/well at room temperature. The culture medium was discarded and replaced with DMEM (Gibco; Thermo Fisher Scientific, Inc.) containing 10 mM H₂-DCFDA (Invitrogen; Thermo Fisher Scientific, Inc.), followed by incubation at 37°C for 30 min. The cells were then washed with PBS and assayed by flow cytometry (FACSCanto II) with BD FACSDiva v8.0.1 software (both from BD Biosciences, San Jose, CA, USA).

Small interfering RNA (siRNA)-targeted gene silencing. Nrf2 siRNA and control (scrambled) siRNA oligonucleotides were synthesized by Shanghai GenePharma Co. Ltd. (Shanghai, China). The sequences are listed in Table I. For siRNA transfection, cells were plated at a density of 1×10^6 cells/well in 24-well plates. At 60% confluence, 30 nM Nrf2 siRNA and 250 μ l Lipofectamine[®] RNAiMAX (Invitrogen; Thermo Fisher Scientific, Inc.) in Opti-MEM were mixed and added to cells in 24-well plates at room temperature. The knockdown efficiencies were assessed by immunoblotting 48 h following siRNA transfection.

Western blot analysis. The cells were lysed with RIPA lysis buffer and mixed with 5X loading buffer. The protein sample was quantified by Bradford assay and was boiled for 10 min and denatured. Each protein sample (50 μ g) was subjected to

10% SDS-PAGE. The separated proteins were transferred onto a PVDF membrane. Following blocking with 5% (w/v) dry non-fat milk in PBS for 2 h at room temperature, the primary antibody was added to the PVDF membrane, followed by overnight incubation at 4°C. Blotting was performed with primary antibody against Nrf2 (cat. no. ab62352; Abcam; 1:1,000 dilution). An HRP-labeled goat-anti-rabbit secondary antibody (cat. no. 7074; Cell Signaling Technology, Inc., Danvers, MA, USA; 1:5,000 dilution) was then applied for 1 h at 37°C. β -actin (cat. no. 4967; Cell Signaling Technology, Inc.; 1:1,000 dilution) and Histone H3 (cat. no. 9715; Cell Signaling Technology, Inc.; 1:1,000 dilution) were used as controls. The membrane was washed three times with TBST, and the blots were developed using an Enhanced Chemiluminescence system (Pierce; Thermo Fisher Scientific, Inc.). ImageJ 1.8.0 (National Institutes of Health, Bethesda, MD, USA) was used to quantify the gray values of each blot.

Reverse transcription-quantitative polymerase chain reaction (RT-qPCR) analysis. Total RNA was extracted using a Universal RNA Extraction kit (Takara Bio, Inc., Otsu, Japan) and reverse transcribed into cDNA with PrimeScript RT Master Mix kit (Takara Bio, Inc., Otsu, Japan). The RT reaction was performed by incubating the samples at 37°C for 15 min, followed by incubation at 85°C for 5 sec and 4°C for 5 min. Equal quantities of cDNA were used for RT-PCR analysis with a SYBR Premix Ex Taq II analysis kit (Takara Bio, Inc.). The thermocycling conditions were as follows: 95°C for 5 min followed by 45 cycles of denaturation at 95°C for 5 sec, annealing at 60°C for 15 sec, and extension at 72°C for 30 sec. qPCR analyses were performed with the Bio-Rad CFX96™ Real-Time PCR detection system and analyzed using CFX™ manager 3.0 (Bio-Rad Laboratories, Inc., Hercules, CA, USA). The specific primers used are listed in Table II. Relative expression levels were normalized to the expression of GAPDH and were quantified using the comparative $2^{-\Delta\Delta C_q}$ method (30).

Flow cytometric analysis of apoptosis. Following digestion with 0.25% trypsin, the primary melanocytes were centrifuged at 800 \times g for 5 min at room temperature and resuspended with 100 μ l binding buffer. Each sample was incubated for 30 min in the dark with 2 μ l Annexin V-FITC and 2 μ l PI staining buffer in binding buffer, following which 300 μ l binding buffer was added to each sample. This was followed by analysis using the FACSCanto II flow cytometer.

Immunofluorescence staining. The NHEMs were seeded on glass slides in a 12-well plate. The glass slides were removed from the 12-well plate and washed twice with PBS. The NHEMs were then fixed with 4% paraformaldehyde for 30 min at room temperature. Following permeabilization by incubation in 0.5% Triton X-100 for 15 min, the NHEMs were blocked with 5% BSA (Beyotime Institute of Biotechnology, Jiangsu, China) at 37°C for 1 h. The cells were then incubated with the primary anti-Nrf2 antibody (1:200 dilution) overnight at 4°C. The cells were washed with PBS five times (3 min each wash) and then incubated with the Alexa Fluor 488-labeled secondary antibody (1:200 dilution) at 37°C for 1 h. The nuclei were counterstained with DAPI. The cells were visualized

under a confocal laser scanning microscope (TCS SP5 II; Leica GmbH, Wetzlar, Germany).

Statistical analysis. Data are presented as the mean \pm SD. Student's t-test was used to analyze differences between two groups. Differences among multiple groups were analyzed by one-way ANOVA with Dunnett's post hoc or Tukey's post hoc test. $P < 0.05$ was considered to indicate a statistically significant difference. Statistical analyses were performed using GraphPad Prism 6.0 (GraphPad Software Inc., San Diego, CA, USA).

Results

GR protects human primary melanocytes against H_2O_2 -induced cell death. The present study investigated the effects of GR (Fig. 1A) on the survival rate and apoptosis of NHEMs treated with H_2O_2 . Our previous study determined that treatment of melanocytes with 0.5 mM H_2O_2 for 24 h was optimal to induce oxidative stress (31). As shown in Fig. 1B, there were no significant changes in cell viability at low doses of GR (0.25, 0.5 and 1 mM), whereas cell viability was significantly lower following treatment with a high dose of GR (1.5 mM) compared with that in untreated cells. When the NHEMs were treated with 1.5 mM GR, the cell survival rate decreased to $48.05 \pm 5.35\%$ compared with that in the untreated cells ($P < 0.05$). Therefore, 1 mM GR was used as the working concentration in the following experiments. The primary human melanocytes were treated with 0.5 mM H_2O_2 in the presence or absence of 1 mM GR, and cell viability was then determined using Cell Counting Kit-8 (CCK-8) assays. Following treatment with 0.5 mM H_2O_2 for 24 h, morphological observation (Fig. 1D-a-d) revealed the melanocyte dendrites were shortened or had disappeared (Fig. 1D-b), and cell viability was decreased to $48.23 \pm 7.25\%$ compared with that in the control cells (Fig. 1C). However, pretreatment with 1 mM GR significantly attenuated H_2O_2 -induced oxidative damage, as represented by an increase of cell viability to $82.7 \pm 5.45\%$ compared with that in control cells (Fig. 1C). In addition, the NHEMs were pretreated with 1 mM GR for 24 h prior to 0.5 mM H_2O_2 treatment and melanocyte apoptosis was then examined using flow cytometry. As shown in Fig. 1E and F, following H_2O_2 treatment, the percentage of apoptotic cells increased to 17.5%, compared with 4.5% in the control group, whereas pretreatment with 1 mM GR markedly inhibited H_2O_2 -induced apoptotic death, with the percentage of Annexin V-stained cells at 8.8%.

GR inhibits H_2O_2 -induced ROS production. The present study subsequently examined whether glycyrrhizin protected melanocytes against oxidative stress. The effects of GR on ROS were measured in NHEMs treated with H_2O_2 . The ROS level was measured using the probe H2-DCFH-DA. As shown in Fig. 2, following H_2O_2 treatment, there was an increase in the level of DCF fluorescence, and the ROS level in NHEMs was significantly reduced by GR pretreatment.

Activation of Nrf2 and induction of HO-1 by GR. To examine the molecular mechanism underlying the effect of GR in reducing oxidative stress, the present study determined

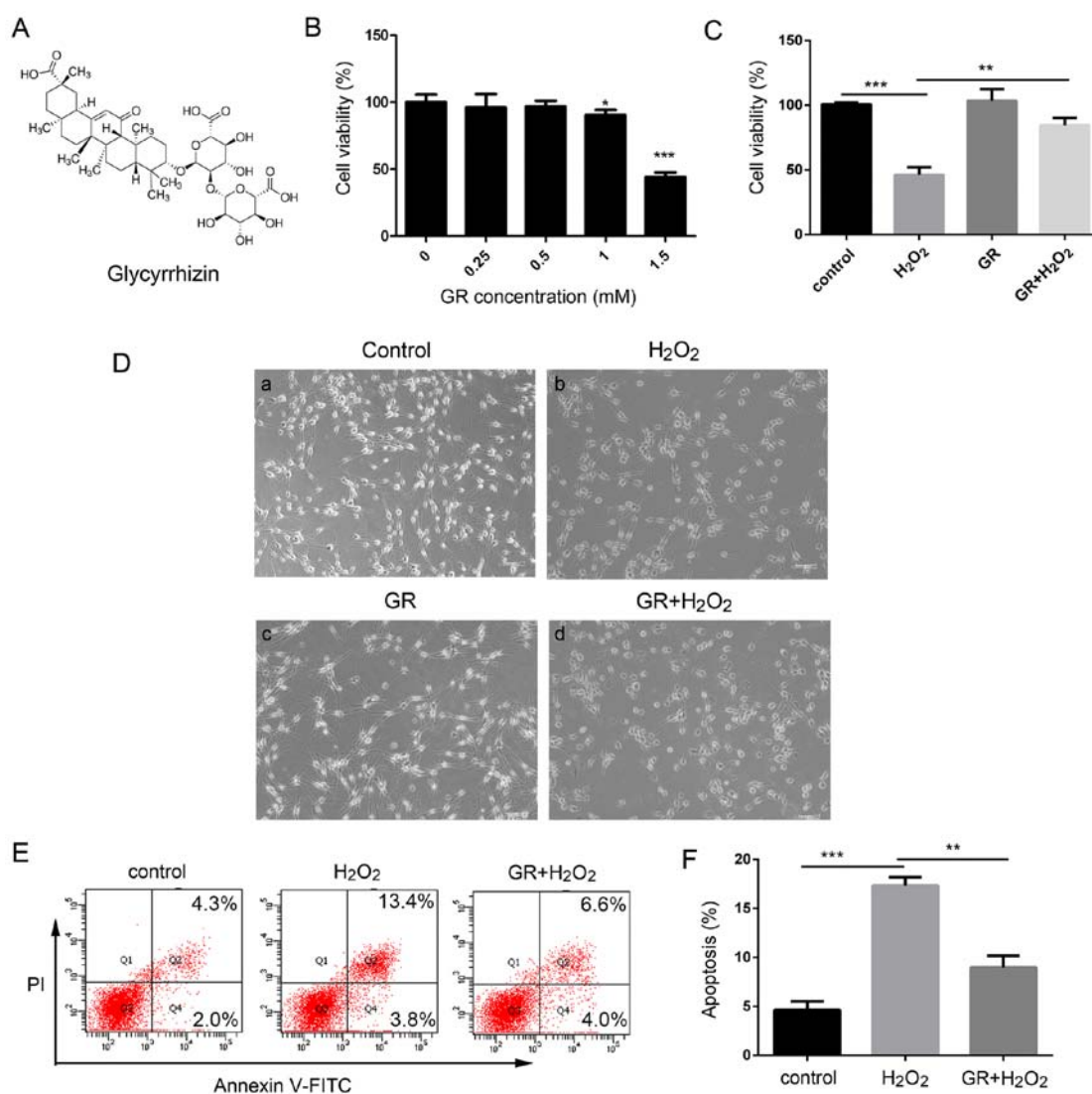


Figure 1. Protective effects of GR against H₂O₂-induced cytotoxicity and apoptosis in NHEMs. (A) Chemical structure of GR. (B) NHEMs were exposed to GR at the indicated concentrations for 24 h, and cell viability was determined using CCK8 assays. (C) NHEMs were pretreated with 1 mM GR for 24 h. Following pretreatment, the cells were treated with 0.5 mM H₂O₂ for 24 h, and cell viability was determined using CCK-8 assays. (D) Effect of GR on H₂O₂-induced morphological changes in primary human melanocytes (x200 magnification). (E) NHEMs were pretreated with or without 1 mM GR for 24 h and then incubated in the presence or absence of 0.5 mM H₂O₂ for 24 h. Apoptosis was assayed by Annexin V-FITC and PI staining, and then analyzed by flow cytometry. (F) Apoptotic rates of NHEMs. Data were obtained from three independent assays and are expressed as the mean \pm SD. ***P*<0.01 vs. H₂O₂ group; ****P*<0.001 vs. control group. NHEMs, normal human epidermal melanocytes; GR, glycyrrhizin; H₂O₂, hydrogen peroxide; PI, propidium iodide; CCK-8, Cell Counting Kit-8.

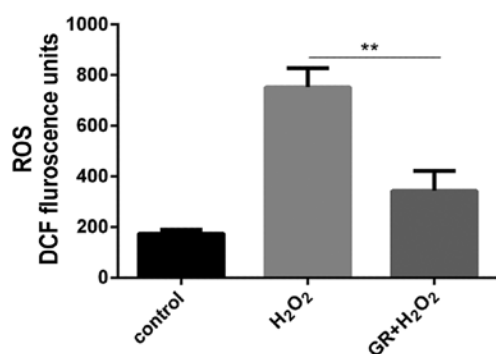


Figure 2. Inhibitory effect of GR on H₂O₂-induced ROS production in NHEMs. NHEMs were pretreated with 1 mM GR and then exposed to 0.5 mM H₂O₂ for 24 h. The ROS level was determined by analysis of H2DCF-DA fluorescence using flow cytometry. Data were obtained from three independent experiments. ***P*<0.01. NHEMs, normal human epidermal melanocytes; GR, glycyrrhizin; H₂O₂, hydrogen peroxide; ROS, reactive oxygen species.

whether GR treatment activated the classical antioxidant pathway of Nrf2. As shown in Fig. 3A, Nrf2 was mainly localized in cytoplasm of the untreated NHEMs. However, in cells treated with GR for 24 h, the expression of Nrf2 in the nucleus was markedly increased. To confirm the nuclear translocation of Nrf2, cytoplasmic and nuclear protein fractions of NHEMs were extracted and immunoblotted with an antibody against Nrf2 (Fig. 3B and C). The expression of Nrf2 was increased significantly following GR treatment, which was consistent with the results of the immunofluorescence. Subsequently, the effects of GR on the expression levels of four downstream genes of the Nrf2 antioxidant pathway were examined. As shown in Fig. 3D, GR treatment increased the expression levels of the four genes, of which the expression of HO-1 was highly elevated.

Subsequently, the primary melanocytes were transfected with Nrf2 siRNAs. Three sequences of Nrf2 siRNAs were used

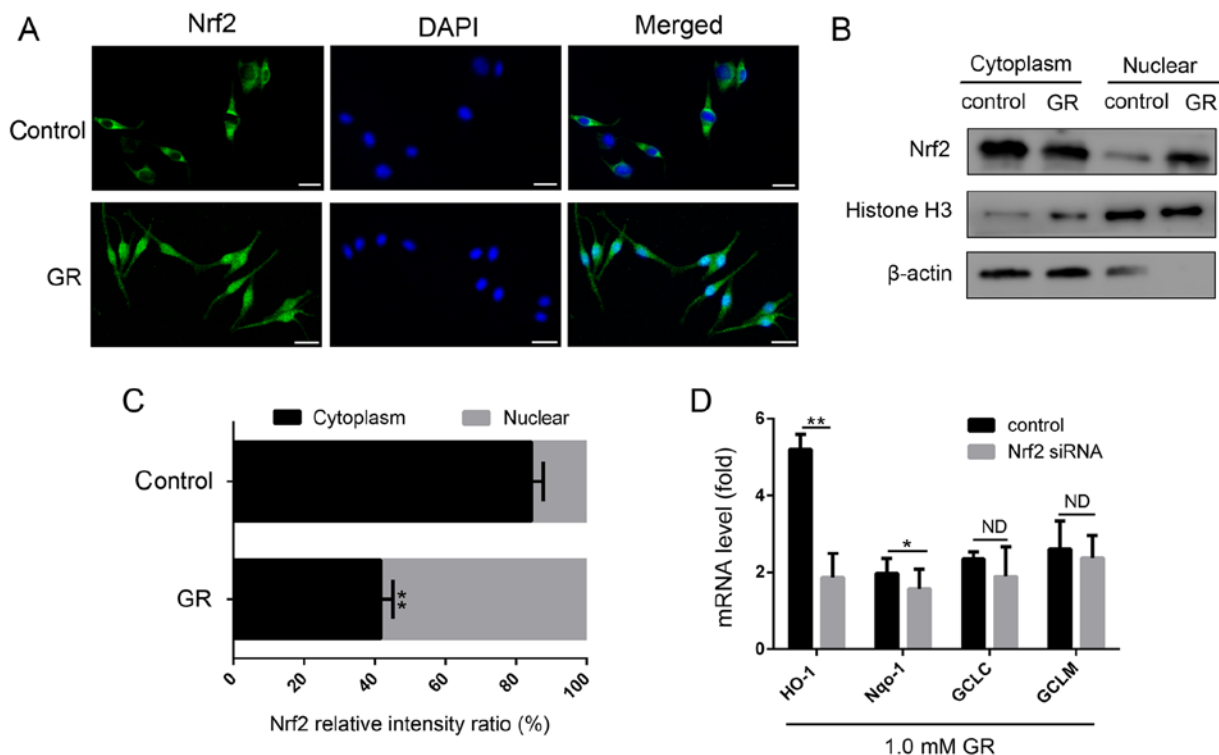


Figure 3. Influence of GR on the activation of Nrf2 and expression of its target genes. (A) Nrf2 immunofluorescence was examined by confocal microscopy following treatment of cells with 1.5 mM GR for 24 h (x400 magnification). Nrf2 was immunostained with an Nrf2-specific antibody (green), and DAPI was used to stain the nucleus (blue). Scale bar=25 μ m. (B) NHEMs were stimulated with 1.5 mM GR for 24 h, following which Nrf2 in cytoplasmic and nuclear protein fractions were detected by western blot analysis and (C) quantified. Histone H3 and β -actin were used as internal references for nuclear and cytoplasmic proteins, respectively. (D) NHEMs were transfected with Nrf2 siRNA or scrambled siRNA for 48 h. mRNA levels of Nrf2 downstream antioxidant genes (HO-1, NQO-1, GCLC and GCLM) were detected by reverse transcription-quantitative polymerase chain reaction analysis. Data are shown as gene expression following normalization to the expression of GAPDH. * $P<0.05$ and ** $P<0.01$ compared with the control. NHEMs, normal human epidermal melanocytes; Nrf2, nuclear factor E2-related factor 2; GR, glycyrrhizin; siRNA, small interfering RNA; HO-1, heme oxygenase-1; NQO-1, NADH quinone oxidoreductase 1; GCLC, glutamate cysteine ligase catalytic subunit; GCLM, glutamyl cysteine ligase modulator subunit; ND, no difference.

Table I. Sequences of siRNAs for Nrf2.

| Name | Sequence (5'-3') |
|-----------------|--|
| Scrambled-siRNA | F: UUCUCCGAACGUGUCACGUTT R: ACGUGACACGUUCGGAGAATT |
| Nrf2(1) | F: GGGAGGAGCUAUUAUCCAUTT R: AUGGAUAAUAGCUCCUCCCTT |
| Nrf2(2) | F: GCCCAUUGAUGUUUCUGAUTT R: AUCAGAAACAUAUAGGGCTT |
| Nrf2(3) | F: CCCGUUUGUAGAUGACAAUTT R: AUUGUCAUCUACAAACGGGTT |

F, forward; R, reverse; Nrf2, nuclear factor E2-related factor 2; siRNA, small interfering RNA.

for knockdown. The Nrf2 knockdown efficiency was evaluated by western blotting and RT-qPCR analysis (Fig. 4). The most efficient sequence was the Nrf2 (3) siRNA. The expression of HO-1 was significantly decreased following transfection with Nrf2 (3) siRNA, whereas the expression of the three other genes was not decreased significantly. Therefore, GR exerted antioxidant effects on melanocytes mainly through the Nrf2-mediated induction of HO-1.

Table II. Primer sequences for polymerase chain reaction.

| Gene | Sequences (5'-3') |
|-------|--|
| Nrf2 | F: CTTGGCCTCAGTGATTCTGAAGTG R: CCTGAGATGGTGACAAGGGTTGTA |
| HO-1 | F: CAGGAGCTGCTGACCCATGA R: AGCAACTGTGCGCCACCAGAA |
| NQO-1 | F: GGATTGGACCGAGCTGGAA R: AATTGCAGTGAAGATGAAGGCAAC |
| GCLC | F: GAAGTGGATGTGGACACCAGATG R: TTGTAGTCAGGATGGTTTGCGATAA |
| GCLM | F: GGAGTTCCCAAATCAACCCAGA R: TGCATGAGATACAGTGCATTCCAA |
| GAPDH | F: ATGACATCAAGAAGGTGGTG R: CATAACAGGAATGAGCTTG |

F, forward; R, reverse; Nrf2, nuclear factor E2-related factor 2; HO-1, heme oxygenase-1; NQO-1, NADH quinone oxidoreductase 1; GCLC, glutamate cysteine ligase catalytic subunit; GCLM, glutamyl cysteine ligase modulator subunit.

Nrf2 knockdown reverses the protective effect of GR on melanocytes against H_2O_2 -induced cytotoxicity. The present study

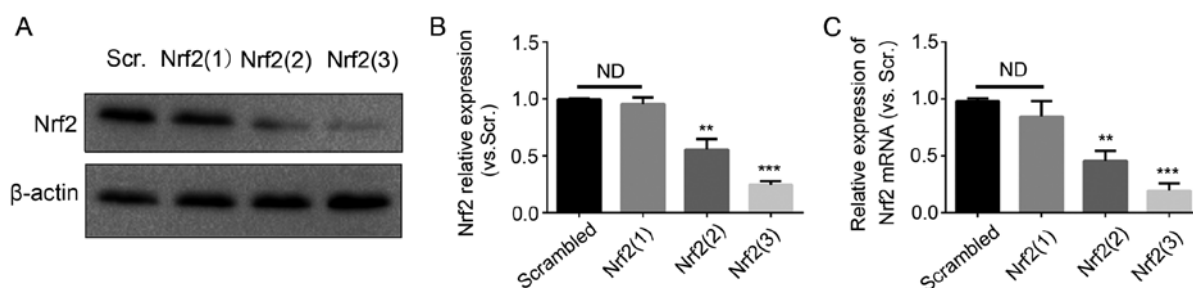


Figure 4. Interference efficiency of three Nrf2-siRNAs. Normal human epidermal melanocytes were transfected with three Nrf2 siRNAs for 48 h, the expression of Nrf2 was confirmed by (A) western blot analysis with (B) quantification, and (C) reverse transcription-quantitative polymerase chain reaction analysis. Scrambled RNA was used as a control. Results are from three independent experiments. ** $P < 0.01$ and *** $P < 0.001$ vs. scrambled siRNA. Nrf2, nuclear factor E2-related factor 2; GR, glycyrrhizin; siRNA, small interfering RNA; Scr, scrambled; ND, no difference.

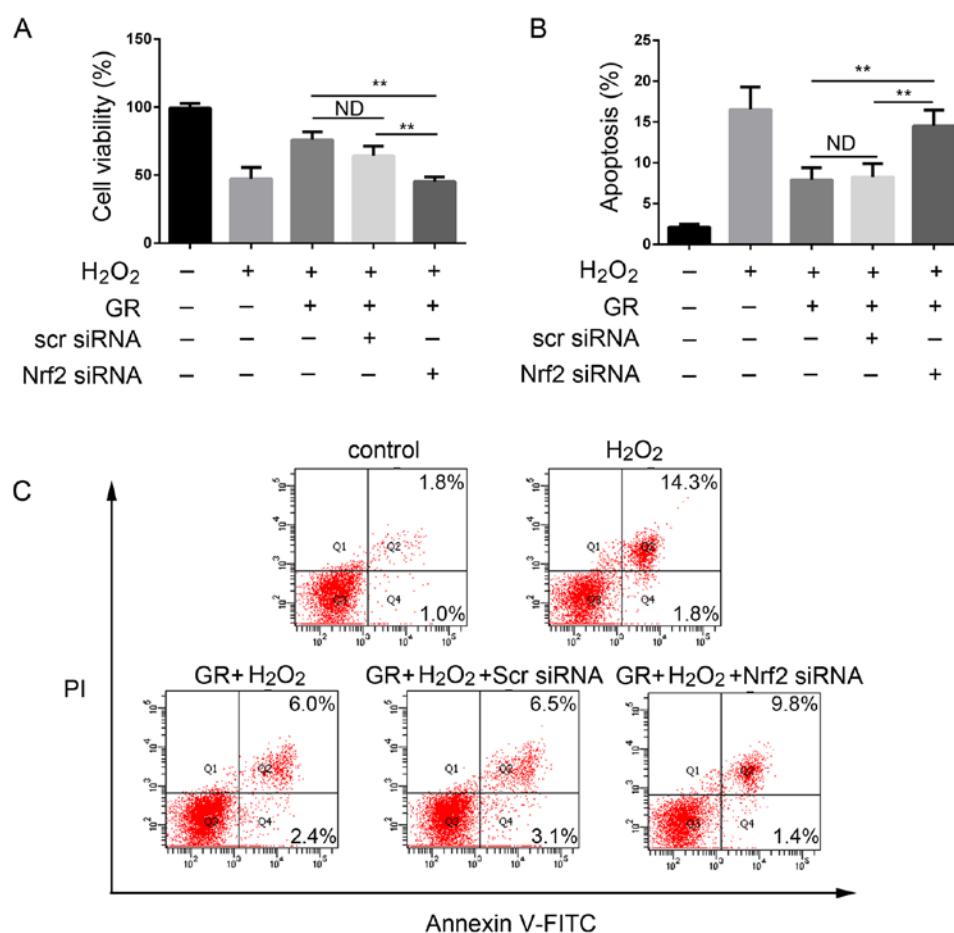


Figure 5. Knockdown of the Nrf2 gene reduces the effect of GR. Normal human epidermal melanocytes were pretreated with Nrf2 siRNA, scr siRNA, and/or GR. (A) viability was assayed using the Cell Counting Kit-8 method at 24 h and (B) apoptosis was examined by flow cytometry following exposure to 0.5 mM H₂O₂. (C) Representative flow cytometry results. Data were obtained from three independent experiments. ** $P < 0.01$. GR, glycyrrhizin; Nrf2, nuclear factor E2-related factor 2; H₂O₂, hydrogen peroxide; siRNA, small interfering RNA; scr, scrambled; PI, propidium iodide; ND, no difference.

then examined whether Nrf2 has a direct role in the antioxidant effect of GR. The NHEMs were first transfected with Nrf2 siRNA or scrambled siRNA for 48 h, followed by 0.5 mM H₂O₂ treatment in the presence of 1 mM GR for 24 h. As shown in Fig. 5A, the viability of the NHEMs was significantly decreased following silencing of Nrf2 compared with that of cells in the control group. Transfection with scrambled siRNA had no cytoprotective effect; cell viability was comparable with that of cells treated with H₂O₂ and GR. GR pretreatment had a significant protective effect on NHEMs, and the apoptotic rate

of the cells was decreased. When the Nrf2 gene was knocked down, the protective effect of GR was decreased significantly (Fig. 5B and C). The cells treated with scrambled siRNA exhibited no changes in GR-induced apoptotic rate under H₂O₂ treatment.

Protective effect of GR on the cytotoxicity and oxidative stress induced by H₂O₂ requires HO-1. To determine the role of the increased expression of HO-1 in the antioxidative effect of GR on melanocytes, the NHEMs were treated with ZnPP, an

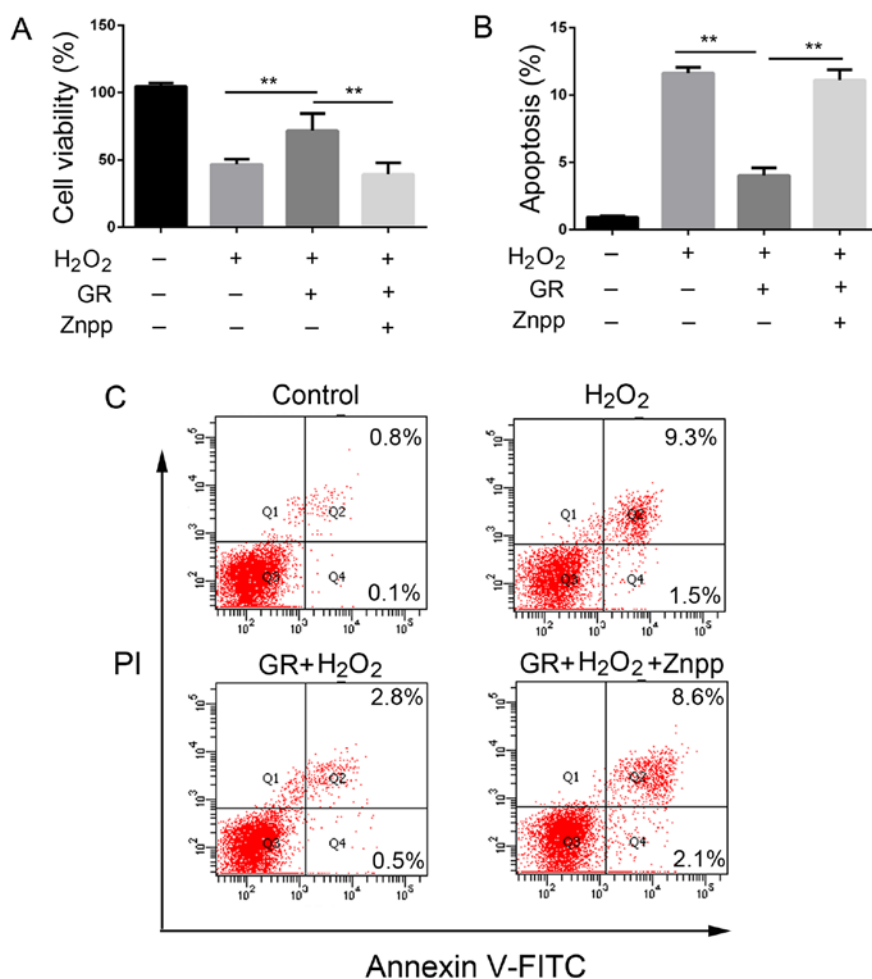


Figure 6. Inhibition of HO-1 by ZnPP reverses the protective effect of GR. (A) Viability of normal human epidermal melanocytes pretreated with ZnPP and/or 1 mM GR was determined using Cell Counting Kit-8 assays at 24 h following exposure to 1 mM H₂O₂. (B) Apoptosis of the cells was examined by (C) flow cytometry. Data were obtained from three independent experiments. **P<0.01. GR, glycyrrhizin; HO-1, heme oxygenase-1; H₂O₂, hydrogen peroxide; PI, propidium iodide.

inhibitor of HO-1, for 24 h, followed by treatment with H₂O₂ for 24 h. The cells were then treated with GR for another 24 h. As shown in Fig. 6, pretreatment with GR increased the viability of the NHEMs and resulted in a significant decrease of apoptotic cells, whereas the addition of ZnPP reversed the effect of GR by reducing the viability of the NHEMs and increasing apoptotic cells (Fig. 6A-C).

Discussion

At present, the main clinical treatment methods for active generalized vitiligo are narrow-band ultraviolet B light combined with oral cortisone or another hormone therapy, topical glucocorticoids, a calcineurin inhibitor (tacrolimus ointment), and 308 nm excimer laser exposure (32,33). Systemic hormones may be considered for cases of rapid progression (34). However, hormonal side effects should be considered, and reports indicate that the recurrence rate following cortisone treatment is high (35). Therefore, the current treatments for vitiligo are not always effective, and certain treatments are limited to specific types of vitiligo.

Accumulating evidence shows that oxidative stress serves a major role in the pathogenesis of vitiligo. Antioxidant

stress-based therapy is a promising strategy for vitiligo. In the present study, it was found that GR protected human melanocytes from H₂O₂-induced oxidative damage via the Nrf2-dependent induction of HO-1. It has been reported that other natural compounds, including melatonin and its metabolites, protect melanocytes from UVB-induced DNA damage through activation of the Nrf2-dependent pathway (36,37). GR also activates the Nrf2 pathway in other cell types (28). In the present study, it was first demonstrated that GR pretreatment improved the survival rate and reduced the apoptotic rate of melanocytes under oxidative stress. It was subsequently demonstrated that GR also activated the Nrf2 antioxidant pathway in melanocytes, and the gene knockdown of Nrf2 significantly reduced the effect of GR.

GR activated downstream genes of the Nrf2 pathway, and siRNA inhibited Nrf2, suggesting that HO-1 serves an important role in antioxidation. It has been reported that HO-1 is an important Nrf2 downstream gene in the protection of melanocytes from oxidative stress (16). The results obtained in the present study support this finding. Other downstream genes of Nrf2 had no significant effect on the effects of GR. The mechanism underlying the effect of GR through Nrf2/HO-1 remains unclear. GR binds to high-mobility group

box 1 (HMGB1) protein and inhibits its cytokine activities as an HMGB1 inhibitor (38). Our previous study also showed that oxidative stress stimulation triggers autocrine HMGB1 translocation and release from melanocytes, leading to the suppressed expression of Nrf2 and downstream genes, which induces melanocyte apoptosis (31). GR may also upregulate the Nrf2 pathway by inhibiting HMGB1 and is involved in antioxidant effects. The Nrf2-induced expression of HO-1 also inhibits the expression of HMGB1, thereby reducing the incidence of inflammation (39,40). Such Nrf2-HO-1-HMGB1 feedback loops may be mechanisms involved in the effects of GR. The underlying specific mechanisms require further investigation. GR promotes melanogenesis in melanoma cells by increasing tyrosinase activity. A limitation of the present study was that melanogenesis was not assessed in human melanocytes, nor was the effect of GR on tyrosinase activity in melanocytes examined.

In conclusion, to the best of our knowledge, the present study is the first to demonstrate that GR protects melanocytes from oxidative stress by activation of the Nrf2 signaling pathway and inducing the expression of HO-1. Therefore, GR may be a promising novel therapeutic drug for vitiligo.

Acknowledgements

Not applicable.

Funding

This study was supported by grants from the National Natural Sciences Foundation of China (grant nos. 81202352 and 81171504) and the Basic Research Program of Natural Science of Shaanxi Province (grant no. 2017JM8140).

Availability of data and materials

All data generated or analyzed during this study are included in this published article.

Authors' contributions

PL conceived and designed the study. KM, WP, DH, XW, YM and FC performed the experiments, and acquired, analyzed and interpreted the data; PL drafted and edited the manuscript. All authors have read and revised the manuscript.

Ethics approval and consent to participate

The present study was approved by the Research Ethics Board of the First Affiliated Hospital of Xi'an Jiaotong University. All participants provided written informed consent prior to inclusion in the study.

Patient consent for publication

Not applicable.

Competing interests

The authors declare that they have no competing interests.

References

- Slominski AT, Zmijewski MA, Skobowiat C, Zbytek B, Slominski RM and Steketee JD: Sensing the environment: Regulation of local and global homeostasis by the skin's neuro-endocrine system. *Adv Anat Embryol Cell Biol* 212: v, vii, 1-115, 2012.
- Slominski A, Tobin DJ, Shibahara S and Wortsman J: Melanin pigmentation in mammalian skin and its hormonal regulation. *Physiol Rev* 84: 1155-1228, 2004.
- Salman A, Kurt E, Topcuoglu V and Demircay Z: Social anxiety and quality of life in vitiligo and acne patients with facial involvement: A cross-sectional controlled study. *Am J Clin Dermatol* 17: 305-311, 2016.
- Njoo MD and Westerhof W: Vitiligo. Pathogenesis and treatment. *Am J Clin Dermatol* 2: 167-181, 2001.
- Slominski A, Zmijewski MA and Pawelek J: L-tyrosine and L-dihydroxyphenylalanine as hormone-like regulators of melanocyte functions. *Pigment Cell Melanoma Res* 25: 14-27, 2012.
- Krüger C and Schallreuter KU: A review of the worldwide prevalence of vitiligo in children/adolescents and adults. *Int J Dermatol* 51: 1206-1212, 2012.
- Ezzedine K, Eleftheriadou V, Whitton M and van Geel N: Vitiligo. *Lancet* 386: 74-84, 2015.
- Picardo M, Dell'Anna ML, Ezzedine K, Hamzavi I, Harris JE, Parsad D and Taieb A: Vitiligo. *Nat Rev Dis Primers* 1: 15011, 2015.
- Schallreuter KU, Moore J, Wood JM, Beazley WD, Gaze DC, Tobin DJ, Marshall HS, Panske A, Panzig E and Hibberts NA: In vivo and in vitro evidence for hydrogen peroxide (H₂O₂) accumulation in the epidermis of patients with vitiligo and its successful removal by a UVB-activated pseudocatalase. *J Invest Dermatol Symp Proc* 4: 91-96, 1999.
- Mohammed GF, Gomaa AH and Al-Dhubaibi MS: Highlights in pathogenesis of vitiligo. *World J Clin Cases* 3: 221-230, 2015.
- Ma Q: Role of nrf2 in oxidative stress and toxicity. *Annu Rev Pharmacol Toxicol* 53: 401-426, 2013.
- Zhu H, Itoh K, Yamamoto M, Zweier JL and Li Y: Role of Nrf2 signaling in regulation of antioxidants and phase 2 enzymes in cardiac fibroblasts: Protection against reactive oxygen and nitrogen species-induced cell injury. *FEBS Lett* 579: 3029-3036, 2005.
- Villeneuve NF, Lau A and Zhang DD: Regulation of the Nrf2-Keap1 antioxidant response by the ubiquitin proteasome system: An insight into cullin-ring ubiquitin ligases. *Antioxid Redox Signal* 13: 1699-1712, 2010.
- Taguchi K, Motohashi H and Yamamoto M: Molecular mechanisms of the Keap1-Nrf2 pathway in stress response and cancer evolution. *Genes Cells* 16: 123-140, 2011.
- Ichimura Y, Waguri S, Sou YS, Kageyama S, Hasegawa J, Ishimura R, Saito T, Yang Y, Kouno T, Fukutomi T, *et al*: Phosphorylation of p62 activates the Keap1-Nrf2 pathway during selective autophagy. *Mol Cell* 51: 618-631, 2013.
- Jian Z, Li K, Liu L, Zhang Y, Zhou Z, Li C and Gao T: Heme oxygenase-1 protects human melanocytes from H₂O₂-induced oxidative stress via the Nrf2-ARE pathway. *J Invest Dermatol* 131: 1420-1427, 2011.
- Jian Z, Li K, Song P, Zhu G, Zhu L, Cui T, Liu B, Tang L, Wang X, Wang G, *et al*: Impaired activation of the Nrf2-ARE signaling pathway undermines H₂O₂-induced oxidative stress response: A possible mechanism for melanocyte degeneration in vitiligo. *J Invest Dermatol* 134: 2221-2230, 2014.
- Kim JY, Lee H, Lee EJ, Kim M, Kim TG, Kim HP and Oh SH: Keap1 knockdown in melanocytes induces cell proliferation and survival via HO-1-associated β -catenin signaling. *J Dermatol Sci* 88: 85-95, 2017.
- Lee CH, Park SW, Kim YS, Kang SS, Kim JA, Lee SH and Lee SM: Protective mechanism of glycyrrhizin on acute liver injury induced by carbon tetrachloride in mice. *Biol Pharm Bull* 30: 1898-1904, 2007.
- Haleagrahara N, Varkkey J and Chakravarthi S: Cardioprotective effects of glycyrrhizic acid against isoproterenol-induced myocardial ischemia in rats. *Int J Mol Sci* 12: 7100-7113, 2011.
- Tang ZH, Li T, Tong YG, Chen XJ, Chen XP, Wang YT and Lu JJ: A systematic review of the anticancer properties of compounds isolated from Licorice (Gancao). *Planta Med* 81: 1670-1687, 2015.
- Ming LJ and Yin AC: Therapeutic effects of glycyrrhizic acid. *Nat Prod Commun* 8: 415-418, 2013.

23. Xiong H, Xu Y, Tan G, Han Y, Tang Z, Xu W, Zeng F and Guo Q: Glycyrrhizin ameliorates imiquimod-induced psoriasis-like skin lesions in BALB/c mice and inhibits TNF- α -induced ICAM-1 expression via NF- κ B/MAPK in HaCaT cells. *Cell Physiol Biochem* 35: 1335-1346, 2015.
24. Wang Y, Zhang Y, Peng G and Han X: Glycyrrhizin ameliorates atopic dermatitis-like symptoms through inhibition of HMGB1. *Int Immunopharmacol* 60: 9-17, 2018.
25. Lee J, Jung E, Park J, Jung K, Park E, Kim J, Hong S, Park J, Park S, Lee S and Park D: Glycyrrhizin induces melanogenesis by elevating a cAMP level in b16 melanoma cells. *J Invest Dermatol* 124: 405-411, 2005.
26. Mou KH, Han D, Liu WL and Li P: Combination therapy of orally administered glycyrrhizin and UVB improved active-stage generalized vitiligo. *Braz J Med Biol Res* 49, 2016.
27. AboEl-Magd NF, El-Mesery M, El-Karef A and El-Shishtawy MM: Glycyrrhizin ameliorates high fat diet-induced obesity in rats by activating Nrf2 pathway. *Life Sci* 193: 159-170, 2018.
28. Kim YM, Kim HJ and Chang KC: Glycyrrhizin reduces HMGB1 secretion in lipopolysaccharide-activated RAW 264.7 cells and endotoxemic mice by p38/Nrf2-dependent induction of HO-1. *Int Immunopharmacol* 26: 112-118, 2015.
29. Xu C, Liang C, Sun W, Chen J and Chen X: Glycyrrhizic acid ameliorates myocardial ischemic injury by the regulation of inflammation and oxidative state. *Drug Des Devel Ther* 12: 1311-1319, 2018.
30. Livak KJ and Schmittgen TD: Analysis of relative gene expression data using real-time quantitative PCR and the 2⁻($\Delta\Delta$ C(T)) method. *Methods* 25: 402-408, 2001.
31. Mou K, Liu W, Miao Y, Cao F and Li P: HMGB1 deficiency reduces H₂O₂-induced oxidative damage in human melanocytes via the Nrf2 pathway. *J Cell Mol Med* 22: 6148-6156, 2018.
32. Lotti T, Gori A, Zanieri F, Colucci R and Moretti S: Vitiligo: New and emerging treatments. *Dermatol Ther* 21: 110-117, 2008.
33. Lotti T, Buggiani G, Troiano M, Assad GB, Delescluse J, De Giorgi V and Hercogova J: Targeted and combination treatments for vitiligo. Comparative evaluation of different current modalities in 458 subjects. *Dermatol Ther* 21 (Suppl 1): S20-S26, 2008.
34. Wassef C, Lombardi A, Khokher S and Rao BK: Vitiligo surgical, laser, and alternative therapies: A review and case series. *J Drugs Dermatol* 12: 685-691, 2013.
35. Majid I and Imran S: Relapse after methylprednisolone oral minipulse therapy in childhood vitiligo: A 12-month follow-up study. *Indian J Dermatol* 58: 113-116, 2013.
36. Skobowiat C, Brożyna AA, Janjetovic Z, Jeayeng S, Oak ASW, Kim TK, Panich U, Reiter RJ and Slominski AT: Melatonin and its derivatives counteract the ultraviolet B radiation-induced damage in human and porcine skin ex vivo. *J Pineal Res* 65: e12501, 2018.
37. Janjetovic Z, Jarrett SG, Lee EF, Duprey C, Reiter RJ and Slominski AT: Melatonin and its metabolites protect human melanocytes against UVB-induced damage: Involvement of Nrf2-mediated pathways. *Sci Rep* 7: 1274, 2017.
38. Mollica L, De Marchis F, Spitaleri A, Dallacosta C, Pennacchini D, Zamaï M, Agresti A, Trisciuglio L, Musco G and Bianchi ME: Glycyrrhizin binds to high-mobility group box 1 protein and inhibits its cytokine activities. *Chem Biol* 14: 431-441, 2007.
39. Faridvand Y, Nozari S, Vahedian V, Safaie N, Pezeshkian M, Haddadi P, Mamipour M, Rezaie-Nezhad A, Jodati A and Nouri M: Nrf2 activation and down-regulation of HMGB1 and MyD88 expression by amnion membrane extracts in response to the hypoxia-induced injury in cardiac H9c2 cells. *Biomed Pharmacother* 109: 360-368, 2019.
40. Park EJ, Kim YM and Chang KC: Hemin reduces HMGB1 release by UVB in an AMPK/HO-1-dependent pathway in human keratinocytes HaCaT cells. *Arch Med Res* 48: 423-431, 2017.



This work is licensed under a Creative Commons Attribution-NonCommercial-NoDerivatives 4.0 International (CC BY-NC-ND 4.0) License.